

PAPER • OPEN ACCESS

Inter-granular effects at high magnetic fields of cuprate and iron chalcogenide superconducting materials

To cite this article: K Buchkov *et al* 2019 *J. Phys.: Conf. Ser.* **1186** 012004

View the [article online](#) for updates and enhancements.



IOP | ebooks™

Bringing together innovative digital publishing with leading authors from the global scientific community.

Start exploring the collection—download the first chapter of every title for free.

Inter-granular effects at high magnetic fields of cuprate and iron chalcogenide superconducting materials

K Buchkov¹, **M Valkovski**¹, **D Gajda**², **K Nenkov**³, **E Nazarova**¹

¹ Institute of Solid State Physics, Bulgarian Academy of Sciences,
72 Tzarigradsko Chaussee, 1784, Sofia, Bulgaria

² Institute of Low Temperatures and Structure Research, Polish Academy of Sciences,
Okólna 2, 50-422 Wrocław, Poland

³ Leibniz Institute for Solid State and Materials Research, (IFW Dresden),
P.O. Box 2700116, D01171 Dresden, Germany
e-mail: buchkov@issp.bas.bg

Abstract. The weak links effects are one of the main challenges for effective power applications of high temperature superconducting materials. Studies of these effects help for their better understanding and subsequent improvement. An overview analysis of the intergranular properties of cuprate ($Y_{0.8}Ca_{0.2}Ba_2Cu_3O_{7-\delta}$) and iron-based chalcogenide ($FeSe_{0.5}Te_{0.5}$) polycrystalline samples was carried out, by means of series of electro-transport experiments at different magnetic fields. The temperature evolution of the Josephson coupling and intrinsic superconductivity effects for the both systems was constructed. The $FeSe_{0.5}Te_{0.5}$ compound shows very stable and superior behavior compared to $Y_{0.8}Ca_{0.2}BCO$ up to the highest magnetic fields (14T) used. We have explored $FeSe_{0.5}Te_{0.5}$ Josephson weak links influence (as a non-linear process) over the resistive transition using different AC current amplitudes and applying the sensitive AC transport third harmonics technique.

1. Introduction

One of the major obstacles before the high power applications of HTSCs (for both cuprates and iron based superconductors (IBS)) is the prominent weak link effects of the grain boundaries which limits the effective critical current density [1]. The layered crystal structure (especially the cuprates) leads to a highly asymmetrical order parameter (p - d wave) and strong anisotropy of the superconducting properties. Consequently, the electro-transport capabilities are highly dependent on the grain boundaries misorientation angle [2] and the specific materials morphology (size, shape and packing of the grains). In addition, the grain boundaries regions have a specific defect structure and altered local chemical composition and electronic properties [3]. The grain boundaries as natural defects and their variable composition as well changes the electronic mean free path and affects the Ginzburg-Landau parameter and subsequently the pinning strength at boundaries region [4]. Usually, the grain periphery is also oxygen depleted (for the cuprates) and thus may form a SIS type inter-grain junctions (superconductor-insulator-superconductor) [5].

For the IBS there are more advantageous options for the weak link problem, due to reasons such as the semi-metallic nature of the normal state (compared to the antiferromagnetic Mott insulator state for the cuprates) and the s -wave highly symmetric order parameter resulting in a lower anisotropy of the properties [6]. Expectedly, the values of the critical grain misorientation angle and its influence over the current density are effectively superior [7]. In addition the grain boundary junctions for IBS show a metallic behavior resulting in the preferable SNS type connections (superconductor-normal metal-



superconductor) [8]. The overcoming of the high critical current limitation of the weak link in granular type superconductors is one of the most investigated topics. There is a number of developing processing methods: on a first place approaches for morphology texturing control, annealing under hot isostatic pressure (proven effective for IBS and MgB_2) [9,10], chemical modification (substitutions and/or additions) of the grain boundary regions [11,12].

In this study we present a qualitative overview of the weak link behaviour in two HTSC systems in form of polycrystalline samples: the cuprate system – $\text{Y}_{0.8}\text{Ca}_{0.2}\text{Ba}_2\text{Cu}_3\text{O}_{7-\delta}$ and the IBS – $\text{FeSe}_{0.5}\text{Te}_{0.5}$. By means of electro-transport experiments we have analysed the resistive transitions to superconducting state in various set of applied high magnetic fields (H_{DC}) and also amplitudes (I_{AC}) of applied AC transport current particularly for $\text{FeSe}_{0.5}\text{Te}_{0.5}$.

2. Experimental details

The main objects of the present study are two polycrystalline samples: cuprate $\text{Y}(\text{Ca})\text{BCO}$ and IBS $\text{FeSe}_{0.5}\text{Te}_{0.5}$. The preparation details, structural and morphological characterization are presented elsewhere: $\text{Y}(\text{Ca})\text{BCO}$ [13,14] and IBS [15]. The resistive experiments are performed using the AC transport modules of two (9 and 14T) PPMS systems. The samples dimensions: for $\text{Y}_{0.8}\text{Ca}_{0.2}\text{Ba}_2\text{Cu}_3\text{O}_{7-\delta}$ cross section $A = 0.18 \text{ cm}^2$ and voltage leads distance $l = 0.34 \text{ cm}$, for $\text{Y}_{0.975}\text{Ca}_{0.025}\text{Ba}_2\text{Cu}_3\text{O}_{7-\delta}$ $A = 0.24 \text{ cm}^2$, $l = 0.44 \text{ cm}$ and for $\text{FeSe}_{0.5}\text{Te}_{0.5}$, $A = 0.24 \text{ cm}^2$, $l = 0.3 \text{ cm}$

One of the samples - $\text{FeSe}_{0.5}\text{Te}_{0.5}$ was additionally characterized by third harmonics resistive measurements which were challenging from experimental point of view. In order to achieve optimal balance of signal sensitivity and accuracy for the effective third harmonic detection, specific amplitudes and frequencies were selected as well with certain adjustments of the system signal gain settings. For the PPMS the higher harmonics data are acquired in dB referenced to the fundamental component voltage signal. The harmonic contribution is usually less than -50 dB for a clean measurement. For the studied superconducting transition the harmonic signal intensity is within range. While for larger dB range when analysing very small signals, the experimental data could be deformed by false experimental artefacts.

3. Results and discussion

The choice of $\text{Y}_{0.8}\text{Ca}_{0.2}\text{Ba}_2\text{Cu}_3\text{O}_{7-\delta}$ system for the present study is based on a number of effects resulting from the substitution, with specifically strong influence over the inter-granular properties (depending on the percentage of substitution) [16–18]. In particular, the Ca segregates mainly at the grains periphery which changes locally the electronic structure, charge balance, carrier mean free path, pinning and reduces the anisotropy effects [18]. In addition the Ca substitution alters the morphology (resulting in smaller and spherical shaped grains [14]) and leads to improved eutectics by lowering the melting temperature of the compound and more easy possibility for texturing [19]. The weak link type is transformed from SIS (typical for YBCO) to SNS type, the negative effects of the critical mis-orientation angle are reduced and the overall inter-granular transport capabilities are significantly improved [14,20].

Due to the overdoping the normal state resistance is also reduced so the stability of the superconductor in case of quench is also improved. Unfortunately, there are also several important adverse effects of the substitution (which tend to increase with the level of overdoping/substitution), specifically the critical temperature of $\text{Y}_{0.8}\text{Ca}_{0.2}\text{Ba}_2\text{Cu}_3\text{O}_{7-\delta}$ is lower compared to YBCO and the inter-grain transition is shifted to much lower temperatures [14].

From practical view the $\text{FeSe}_{0.50}\text{Te}_{0.50}$ is the most perspective compound of chalcogenide IBS. It is structurally simple (low anisotropy) and chemically stable (in comparison to FeSe and particularly $\text{Re}(\text{A})\text{Fe}_2\text{Se}_2$ systems: Re – rare earth element or A organic radical [21]) and possesses appropriate morphology consisting of compact and partially melted grains (prerequisite for large area of the Josephson contacts). In addition, the structural disorder is in favorable margins as a result of nano-scale phase separation, thus the pinning landscape is very effective due to different types of pinning centers [22]. The critical parameters and particularly the critical current persists up to very high magnetic fields

[23]. This is also as a result from a superior inter-grain current capabilities especially due to the metallic type SNS junctions [8].

The inter-granular properties of polycrystalline $Y_{0.8}Ca_{0.2}Ba_2Cu_3O_{7-\delta}$ sample have been analyzed by series of resistive R vs T experiments at various fixed DC magnetic fields. The results are presented on figure 1 (A) and normally a semi logarithmic scale is used in order to individuate the resistive responses of the intra-grain and weak link contributions (in the margins of experiment noise level $\sim 10^{-6} \Omega$).

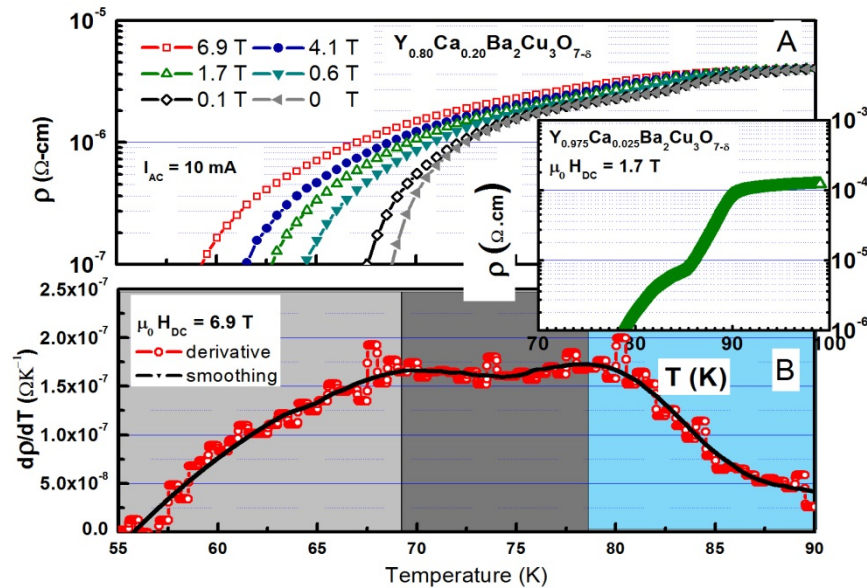


Figure 1. A. Semi logarithmic plot of resistivity vs. temperature for $Y_{0.80}Ca_{0.20}BaCuO$ sample at different magnetic fields. B. Derivative of resistivity vs. temperature for 6.9 T. Inset. Semi logarithmic plot of resistivity vs. temperature for $Y_{0.975}Ca_{0.025}Ba_2Cu_3O_{7-\delta}$ sample at 1.7 T.

For all applied fields the resistive curves have a typical for the intra/inter-grain transitions double step shape. The overall resistive response is dominated by the weak link influence resulting in broadening and shifting of the transitions to lower temperatures with increasing of the applied DC field. The physical phenomenology behind the observed behaviour is well investigated in the literature. It is related with the specific temperature and field evolution of processes in the intrinsic superconductor volume (intra-grain) and the Josephson inter-grain medium [20,24,25]. In order to present the domains of activity of the different transitions, the data are also represented using the $R(T)$ first derivative and marked by the corresponding inflection points (figure 1 B).

At the lowest temperatures (light grey) a stable current percolation path is established through the effectively coupled Josephson links. The rapid increase of the resistance with the temperature is related to penetration of the magnetic flux inside the inter-grain regions (which is controlled by Josephson type vortices). As a consequence the number of non-dissipating (coupled) Josephson contacts (dark grey) decreases till reaching certain limit because the normal state junctions (decoupled) are expected to be independent from the DC field. This is manifested as saturation in the magneto-resistance behaviour. The DC field penetrates also inside the superconducting grains and at the higher temperatures close to T_c , the resistive response is controlled only by the intrinsic vortex dynamics processes (blue area).

For comparison and to emphasize the effect of Ca-substitution on the weak-link behaviour, the $R(T)$ data for sample with a small percentage of substitution (2.5%) are also presented in the inset section of figure 1 for a fixed DC field equal to 1.7T. In this case the transition width (ΔT) is of order of 10K, which is smaller than ΔT for 20% Ca substituted sample, where $\Delta T \sim 30$ K. The higher Ca concentration

increases the number of grain connections (ρ is reduced more than one order of magnitude), but the length scale of boundary imperfection probably exceeds the coherence length and electron mean free path, which is detrimental for some of the pinning centers and broadens the transition.

On figure 2 A the temperature dependence of the resistivity $R(T)$ for polycrystalline $\text{FeSe}_{0.5}\text{Te}_{0.5}$ sample (up to $\mu_0 H_{\text{DC}} = 14\text{T}$ and few are shown for clarity) is presented (semi-logarithmic scale). The resistive curves display slight (about 4K) transition broadening of the (for 14T). The double step transition is observed for all curves but in contrast to the behaviour of $\text{Y}_{0.8}\text{Ca}_{0.2}\text{Ba}_2\text{Cu}_3\text{O}_{7-\delta}$ in moderate DC fields, the inter- and intra-grain responses are far less distinguishable.

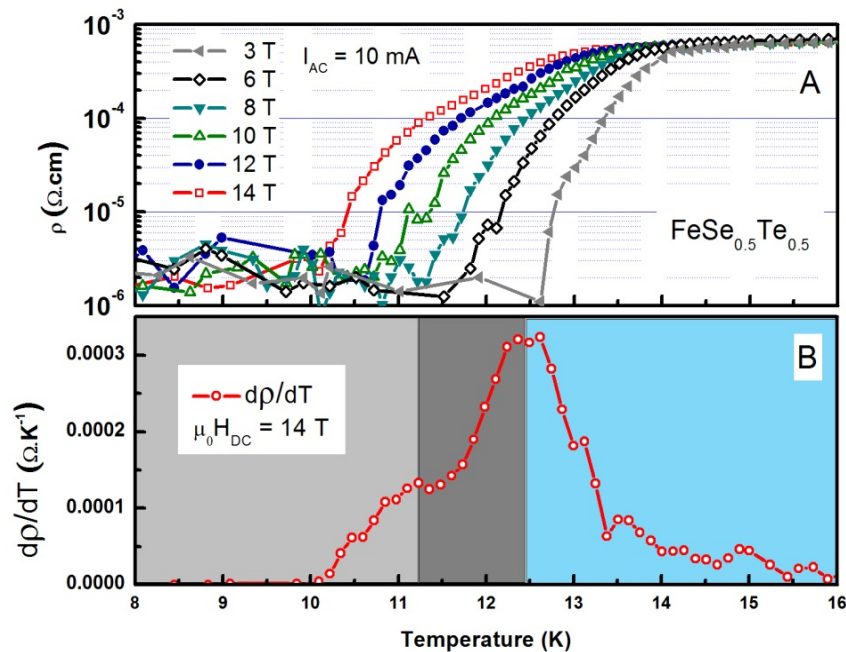


Figure 2. Semi logarithmic plot of resistivity vs. temperature for $\text{FeSe}_{0.5}\text{Te}_{0.5}$ sample at different magnetic fields. B. Derivative of resistivity vs. temperature for 14 T.

The $R(T)$ derivative main peak splitting is detectable only above 10T and the inter- and intra-grain components separation is most prominent for 14T (presented on figure 2(B)). Obviously, for $\text{FeSe}_{0.5}\text{Te}_{0.5}$ the temperature evolution of the current transport through dominating regimes of coupled, decoupled Josephson links and bulk (grain) volume is in very narrow interval. The lower T_c and smaller thermal fluctuations in comparison with $\text{Y}(\text{Ca})\text{BCO}$ contribute for this result.

We have investigated the electro-transport behaviour of $\text{FeSe}_{0.5}\text{Te}_{0.5}$ also from the perspective of AC current amplitude variation (no DC field applied). The results for three different amplitudes (10, 50 and 100mA) are presented on figure 3A using a semi-logarithmic scale. In this case the double step transition is indistinct and hardly visible. It was impossible to directly individuate the inter-grain domain signal via the differentiation routine. The AC transport response of superconductor is very complex due to the combined effects of various linear and non-linear processes [26,27]. The Josephson Effect is a typical example of a non-linear phenomenon and therefore is expected to cause a higher harmonics generation in the AC signal. Usually, the third harmonics modulus $U_{3\omega}$ is studied because of the highest signal allowing sensitive detection of different non-linear processes. The results are presented on figure 3 B. A stable harmonic signal was achieved only for the highest AC current amplitudes (50 and 100mA).

Particularly a double peak of $U_{3\omega}$ ($I_{\text{AC}} = 100\text{mA}$) was detected as a possible fingerprint of the Josephson links activity as the dominating process in the inter-grain domain. The other non-linear

processes with influence are the flux pinning and creep relaxation but naturally they control the response in the intrinsic (intra-grain) superconductor volume.

In conclusion we have presented a general overview of the electro-transport properties in the context of weak link influence for two compounds in polycrystalline form: $Y_{0.8}Ca_{0.2}Ba_2Cu_3O_{7-\delta}$ (cuprate) and $FeSe_{0.5}Te_{0.5}$ (IBS). The $Y_{0.8}Ca_{0.2}Ba_2Cu_3O_{7-\delta}$ inter-grain response is strongly affected by the magnetic field with even moderate intensity. The resistive behaviour evolves through the different temperature intervals of the domination of coupled, decoupled Josephson links and bulk (grain) volume. However this system operates in much higher temperatures compared to IBS.

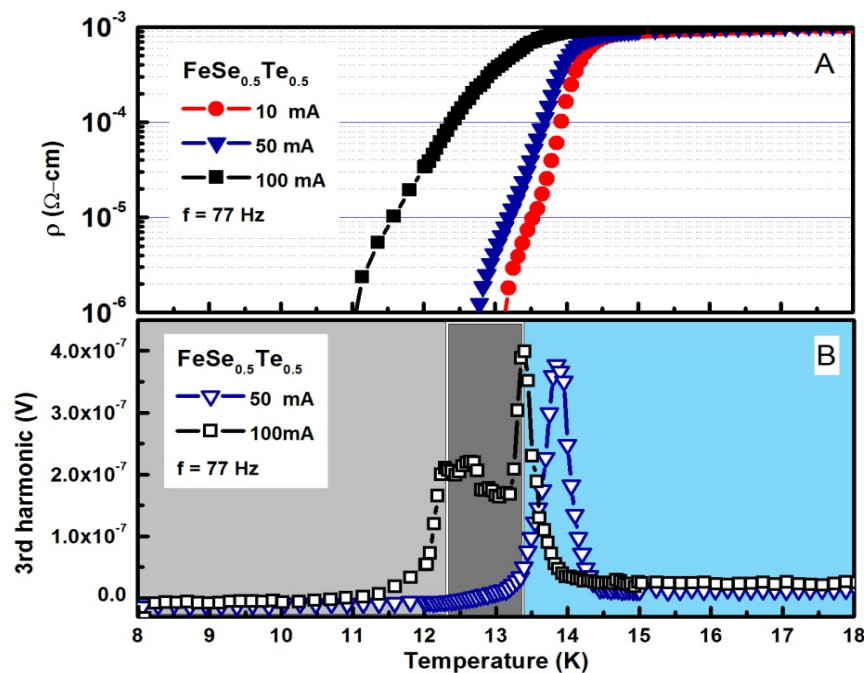


Figure 3. A. Semi logarithmic plot of resistivity vs. temperature for $FeSe_{0.5}Te_{0.5}$ sample at different currents. B. AC transport third harmonic signal vs. temperature for $FeSe_{0.5}Te_{0.5}$ sample at the different AC current amplitudes.

The $FeSe_{0.5}Te_{0.5}$ shows a great stability (in particular for inter-grain) of the resistive transition in very high magnetic fields or current amplitudes (in some extent the intra and inter-grain grain contributions are almost indistinguishable). The Josephson effects influence (as a non-linear phenomenon) over the AC response of $FeSe_{0.5}Te_{0.5}$ was effectively detected by the sensitive third harmonic technique.

Acknowledgments

This work was conducted within the framework of Polish –Bulgarian inter-academical research project.

References

- [1] Hilgenkamp H and Mannhart J 2002 Grain boundaries in high-Tc superconductors *Rev. Mod. Phys.* **74** 485–549
- [2] Dimos D, Chaudhari P and Mannhart J 1990 Superconducting transport properties of grain boundaries in $YBa_2Cu_3O_7$ bicrystals *Phys. Rev. B* **41** 4038–49
- [3] Laval J Y and Swiatnicki W 1994 Atomic structure of grain boundaries in $YBa_2Cu_3O_{7-x}$ *Phys. C Supercond.* **221** 11–9

- [4] Suenaga M and Jansen W 1983 Chemical compositions at and near the grain boundaries in bronze-processed superconducting Nb_3Sn *Appl. Phys. Lett.* **43** 791–3
- [5] Dravid V P, Zhang H and Wang Y Y 1993 Inhomogeneity of charge carrier concentration along the grain boundary plane in oxide superconductors *Phys. C Supercond.* **213** 353–8
- [6] Mazin I I, Singh D J, Johannes M D and Du M H 2008 Unconventional Superconductivity with a Sign Reversal in the Order Parameter of $\text{LaFeAsO}_{1-x}\text{F}_x$ *Phys. Rev. Lett.* **101** 057003
- [7] Katase T, Ishimaru Y, Tsukamoto A, Hiramatsu H, Kamiya T, Tanabe K and Hosono H 2011 Advantageous grain boundaries in iron pnictide superconductors. *Nat. Commun.* **2** 409
- [8] Sarnelli E, Adamo M, Nappi C, Braccini V, Kawale S, Bellingeri E and Ferdeghini C 2014 Properties of high-angle Fe(Se,Te) bicrystal grain boundary junctions *Appl. Phys. Lett.* **104** 162601
- [9] Gajda G, Morawski A, Rogacki K, Cetner T, Zaleski A J, Buchkov K, Nazarova E, Balchev N, Hossain M S A, Diduszko R, Gruszka K, Przystupski P, Fajfrowski Ł and Gajda D 2016 Ag-doped $\text{FeSe}_{0.94}$ polycrystalline samples obtained through hot isostatic pressing with improved grain connectivity *Supercond. Sci. Technol.* **29** 095002
- [10] Gajda D, Morawski A, Zaleski A, Kurnatowska M, Cetner T, Gajda G, Presz A, Rindfleisch M and Tomsic M 2015 The influence of HIP on the homogeneity, J_c , B_{irr} , T_c and F_p in MgB_2 wires *Supercond. Sci. Technol.* **28** 015002
- [11] Glowacki B A 1998 Texture development of HTS powder-in-tube conductors *Supercond. Sci. Technol.* **11** 989–94
- [12] Klie R F, Buban J P, Varela M, Franceschetti A, Jooss C, Zhu Y, Browning N D, Pantelides S T and Pennycook S J 2005 Enhanced current transport at grain boundaries in high- T_c superconductors *Nature* **435** 475–8
- [13] Buchkov K, Nenkov K, Zaleski A, Nazarova E and Polichetti M 2012 Fundamental and 3rd harmonic AC magnetic susceptibility of over-doped polycrystalline $\text{Y}_{1-x}\text{Ca}_x\text{Ba}_2\text{Cu}_3\text{O}_{7-\delta}$ ($x=0.025$ and $x=0.20$) samples *Phys. C Supercond.* **473** 48–56
- [14] Nazarova E, Nenkov K, Zaleski A, Buchkov K and Zahariev A 2012 Investigations of the overdoped state in polycrystalline $\text{R}_{1-x}\text{Ca}_x\text{Ba}_2\text{Cu}_3\text{O}_{7-\Delta}$ samples ($\text{R}=\text{Y}, \text{Eu}, \text{Gd}, \text{Er}$) *Superconductivity: Theory, Materials and Applications* (Nova Science Publishers, Inc.) pp 327–61
- [15] Sedky A, Nazarova E, Nenkov K and Buchkov K 2017 A Comparative Study Between Electro and Magneto Excess Conductivities in FeTeSe Superconductors *J. Supercond. Nov. Magn.* **30** 2751–62
- [16] Cheng C H and Zhao Y 2007 Repair of grain boundary by preferential-doping in $\text{YBa}_2\text{Cu}_3\text{O}_{7-y}$ *Phys. C Supercond. its Appl.* **463–465** 174–7
- [17] Berenov A, Farvacque C, Qi X, MacManus-Driscoll J., MacPhail D and Foltyn S 2002 Ca doping of YBCO grain boundaries *Phys. C Supercond.* **372–376** 1059–62
- [18] Laval J Y and Orlova T S 2002 Microstructure and superconducting properties of sintered DyBaCuO ceramics doped by Ca *Supercond. Sci. Technol.* **15** 314
- [19] Buchkov K, Nazarova E, Gurova K, Zahariev A, Sechenski H and Nenkov K 2012 Reduction of YBCO melting temperature by simultaneous Ca substitution and Ag addition *Optoelectron. Adv. Mater. Rapid Commun.* **6** 1061–3
- [20] Schmehl A, Goetz B, Schulz R R, Schneider C W, Bielefeldt H, Hilgenkamp H and Mannhart J 1999 Doping-induced enhancement of the critical currents of grain boundaries in $\text{YBa}_2\text{Cu}_3\text{O}_{7-\delta}$ *Europhys. Lett.* **47** 110–5
- [21] Krzton-Maziopa A, Pomjakushina E V, Pomjakushin V Y, von Rohr F, Schilling A and Conder K 2012 Synthesis of a new alkali metal-organic solvent intercalated iron selenide superconductor with $T_c \approx 45$ K. *J. Phys. Condens. Matter* **24** 382202
- [22] Rößler S, Cherian D, Harikrishnan S, Bhat H L, Elizabeth S, Mydosh J A, Tjeng L H, Steglich F and Wirth S 2010 Disorder-driven electronic localization and phase separation in superconducting $\text{Fe}_{1+y}\text{Te}_{0.5}\text{Se}_{0.5}$ single crystals *Phys. Rev. B* **82** 144523

- [23] Lei H, Wang K, Hu R, Ryu H, Abeykoon M, Bozin E S and Petrovic C 2012 Iron chalcogenide superconductors at high magnetic fields *Sci. Technol. Adv. Mater.* **13** 054305
- [24] Ekin J W, Braginski A I, Panson A J, Janocko M A, Capone D W, Zaluzec N J, Flandermeyer B, de Lima O F, Hong M, Kwo J and Liou S H 1987 Evidence for weak link and anisotropy limitations on the transport critical current in bulk polycrystalline $\text{YBa}_2\text{Cu}_3\text{O}_x$ *J. Appl. Phys.* **62** 4821–8
- [25] Vanderbemden P, Bradley A D, Doyle R A, Lo W, Astill D M, Cardwell D A and Campbell A M 1998 Superconducting properties of natural and artificial grain boundaries in bulk melt-textured YBCO *Phys. C Supercond.* **302** 257–70
- [26] Cheenne N, Mishonov T and Indekeu J O 2003 Observation of a sharp lambda peak in the third harmonic voltage response of high- T_c superconductor thin films *Eur. Phys. J. B - Condens. Matter* **32** 437–44
- [27] Ossandón J G, Giordano J L, Esquinazi P, Kempa K, Schaufuss U and Sergeenkov S 2006 Non-linear response of ac conductivity in narrow YBCO film strips at the superconducting transition *J. Phys. Conf. Ser.* **43** 655–8